Characterization and Catalytic Activity of Gold Nanoparticles Synthesized by Autoreduction of Aqueous Chloroaurate Ions with Fumed Silica

Priyabrata Mukherjee,[†] Chitta Ranjan Patra,[†] Anirban Ghosh,[†] Rajiv Kumar,*[,†] and Murali Sastry*[,‡]

Catalysis and Materials Chemistry Divisions, National Chemical Laboratory, Pune 411 008, India

Received September 12, 2001. Revised Manuscript Received January 2, 2002

In this report, a novel method for the synthesis of gold nanoparticles on an amorphous silica support is described wherein silanol groups on the surface of the fumed silica spontaneously reduce aqueous chloroaurate ions. This results in the formation of gold nanoparticles that are bound fairly strongly to the fumed silica surface. Alkylamine molecules present in solution were observed to reduce the size of the gold nanoparticles thus formed by self-assembling on the nanoparticles and preventing further growth. The gold nanoparticle size is dependent on the concentration of alkylamine molecules in solution. The gold nanoparticle−fumed silica composite material was found to be catalytically active in the hydrogenation of cyclohexene.

Introduction

During the past decade or so, much effort has been directed toward understanding the physical and chemical properties of nanoparticles because of their immense importance in catalysis[1] and optoelectronic applications[2] and as templates for biominerals,[3] to mention a few applications. Recently, interest has been renewed in the synthesis of organic−inorganic[4] and inorganic−inorganic nanocomposite materials.[5] In all of the above cases, the hosts are usually passive and do not participate in the reduction of the metal ions to form the metal nanoparticles. There are few reports in the literature, barring those of Esumi et al.[6a] and Mukherjee et al.,[6b,c] wherein the host has been found to participate actively in the reduction of metal ions to form metal nanoparticles, which are then entrapped in the host matrix. Realizing the immense importance of nanocomposites in future applications, we have developed a novel method for the synthesis of gold nanoparticles by the spontaneous reduction of aqueous chloroaurate ions ($AuCl_4^-$) by fumed silica. We also show that it is possible to control the size of the gold nanoparticles formed on the surface of the fumed silica through the presence of alkylamine molecules in solution, with the particle size depending on the concentration of the alkylamine compound in solution. It is known that primary amines bind to the surface of gold nanoparticles via covalent linkages,[7] and we have recently used this approach to develop a protocol for the phase transfer of aqueous gold nanoparticles into nonpolar organic phases,[8] as well as for the capping of gold nanoparticles with amino acid molecules to render them amphoteric.[9] The amine molecules thus self-assemble on the surface of the gold nanoparticles as the metal ions are reduced by the fumed silica and prevent further growth beyond the initial stage of nucleation. This leads to smaller gold particles on the fumed silica surface and might be a possible strategy for the size control of the gold nanoparticles using amines along the lines developed using alkanethiols.[10] The Au nanoparticle−fumed silica material is an example of inorganic−inorganic nanocomposites wherein the matrix actively participates in the reduction of the metal ions, as well as acting as a support for the nanoparticles thus formed. We also demonstrate the catalytic application of this nanocomposite in the hydrogenation of cyclohexene.

Experimental Details

1. Materials. Fumed silica (Aldrich, surface area 384 m^2 g^{-1}), chloroauric acid (SD Fine Chem, India), dodecylamine

* Authors to whom all correspondence should be addressed. E-mail: rajiv@cata.ncl.res.in and sastry@ems.ncl.res.in.

[†] Catalysis Division.

[‡] Materials Chemistry Division.

(1) (a) Haruta, M. *Catal. Today* **1997**, *36*, 153. (b) Valden, M.; Lai, X.; Goodman, D. W. *Science* **1998**, *281*, 1647. (c) Bond, G. C.; Thompson, D. T. *Catal. Rev.−Sci. Eng.* **1999**, *41*, 319.

(2) (a) Gracias, D. H.; Tien, J.; Breen, T. L.; Hsu, C.; Whitesides, G. M. *Science* **2000**, *289*, 1170. (b) Collier, C. P.; Mattersteig, G.; Wong, E. W.; Luo, Y.; Beverly, K.; Sampio, J.; Raymo, F. M.; Stoddart, J. F.; Heath, J. R. *Science* **2000**, *289*, 1172.

(3) Kunther, J.; Seshadri, R.; Nelles, G.; Assenmacher, W.; Butt, H.-J.; Mader, W.; Tremel, W. *Chem. Mater.* **1999**, *11*, 1317.

(4) (a) Beecroft, L. L.; Ober, C. K. *Chem. Mater.* **1997**, *9*, 1302. (b) Shenton, W.; Pum, D.; Sleytr, U. B.; Mann, S. *Nature* **1997**, *389*, 585. (c) Sastry, M. *Curr. Sci.* **2000**, *72*, 1089. (d) Zhao, M.; Sun, L.; Crooks, R. M. *J. Am. Chem. Soc.* **1998**, *120*, 4877.

(5) (a) Mukherjee, P.; Sastry, M.; Kumar, R. *Phys. Chem. Commun.* **2000**, 4. (b) Hirai, T.; Okubo, H.; Komasawa, I. *J. Phys. Chem. B* **1999**, *103*, 4228.

(6) (a) Esumi, K.; Hosoya, T.; Suzuki, A.; Torigoe, K. *Langmuir* **2000**, *16*, 2978. (b) Mukherjee, P.; Patra, C. R.; Kumar, R.; Sastry, M. *Phys. Chem. Commun.* **2001**, *5*, 1. (c) Mukherjee, P.; Ahmad, A.; Mandal, D.; Senapati, S.; Sainkar, S. R.; Khan, M. I.; Ramani, R.; Parischa, R.; Ajayakumar, P. V.; Alam, M.; Sastry, M.; Kumar, R. *Angew. Chem., Int. Ed. Engl.* **2001**, *40*, 3585.

(7) Leff, D. V.; Brandt, L.; Heath, J. R. *Langmuir* **1996**, *12*, 4723.

(8) Sastry, M.; Kumar, A.; Mukherjee, P. *Colloids Surf. A* **2001**, *181*, 255.

(9) Kumar, A.; Mukherjee, P.; Guha, A.; Adyanthaya, S. D.; Mandale, A. B.; Kumar, R.; Sastry, M. *Langmuir* **2000**, *16*, 9775.

(10) Leff, D. V.; Ohara, P. C.; Heath, J. R.; Gelbart, W. M. *J. Phys. Chem.* **1995**, *99*, 7036.

10.1021/cm010372m CCC: $22.00
Published on Web 03/09/2002

Scheme 1. Hydrogenation of Cyclohexene

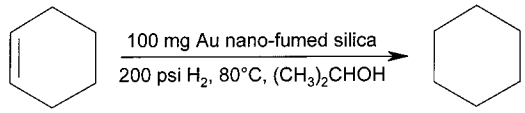

(SRL, India), and cyclohexene (Thomas Baker, India) were used as received.

2. Instruments. The UV−vis spectra of all of the samples were measured on a Shimadzu UV-2101PC spectrophotometer operating in the reflection mode at a resolution of 2 nm using barium sulfate as the standard for background correction. X-ray diffraction (XRD) patterns were recorded on a Phillips PW 1830 instrument operating at a voltage of 40 kV and a current of 30 mA with Cu K_α radiation. Transmission electron microscopy (TEM) measurements were carried out on a JEOL model 1200EX instrument operated at an accelerating voltage of 120 kV. Thermogravimetry (TGA) and differential thermal analysis (DTA) measurements were carried out on a Seiko Instruments model TG/DTA 32 instrument at a heating rate of 10°/min. Energy dispersive X-ray (EDX) analyses were performed with Kevex equipment attached to a JEOL JSM-5200 scanning microscope.

3. Preparation of Au Nanoparticle−Fumed Silica Samples. Fumed silica samples with different concentrations of surface hydroxyl groups were prepared by reacting 0.5 g of fumed silica with 50 mL of 5% HCl for 0 h (sample 1), 1 h (sample 2), 6 h (sample 3), 12 h (sample 4), and 24 h (sample 5). These samples of fumed silica were then filtered, washed thoroughly with water, and dried prior to reaction with gold ions. The concentration of free hydroxyl groups in the different fumed silica samples was determined by a modified Fripiat and Uytterhoeven method,[11] according to which fumed silica was treated with methylmagnesium iodide in dibutyl ether under nitrogen atmosphere and the evolved methane gas was measured.

The autoreduction of gold ions in fumed silica samples 1−5 was carried out in a 100-mL round-bottom flask in which 0.5 g of fumed silica was reacted with 50 mL of an aqueous solution of 10^{-4} M $HAuCl_4$ and kept under continuous stirring for 40 h at room temperature. To determine whether the size of the gold nanoparticles could be controlled using this process, similar experiments were carried out with fumed silica sample 5 and 10^{-4} M aqueous $HAuCl_4$ solution containing the following concentrations of dodecylamine (DDA) molecules: (i) 10^{-1} M (designated as SiAuD1), (ii) 10^{-3} M (designated as SiAuD3), and (iii) 10^{-6} M (designated as SiAuD6, listed in Table 2 below). The amine molecules were solubilized in the gold ion solution using 1 mL of ethanol. After 40 h of stirring, the samples were filtered, washed repeatedly with distilled water, and dried under suction at ambient temperature; they were then stored in a desiccator. A small amount of the autoreduced gold sample 5 (designated as SiO_2−Au) was heated at 400 °C for 1 h to study the effect of heating on the size and packing density of the gold nanoparticles on the silica surface (sample 6, designated as SiAu400).

4. Hydrogenation of Cyclohexene. The hydrogenation reactions (see Scheme 1) were carried out in a 300 mL pressure autoclave at 80 °C and under 200 psi of H_2 for 90 min, where 100 mg of the Au nanoparticle−fumed silica composite materials were individually treated with 10 mL of cyclohexene in 90 mL of 2-propanol. Samples of the reaction mixture were removed out at different time intervals and analyzed by capillary gas chromatography using a flame ionization detector.

Results and Discussion

The values of the surface hydroxyl group concentrations in fumed silica samples 1−5 prepared in the manner detailed above are listed in Table 1. It can be clearly seen in Table 1 that the surface hydroxyl concentration increases uniformly as the time of reaction of fumed silica with HCl increases. The Au/Si weight ratios (from EDX measurements) are also listed in the same table, from which it is evident that the concentration of gold on the silica surface increases with increasing number of surface hydroxyl groups (Table 1, samples 1−5).

Table 1. Au Content and Concentration of Free Hydroxyl Groups on the Surfaces of Different Fumed Silica Samples

time of HCl treatment (h)	sample	Au/Si (wt/wt)	no. of free hydroxyl groups (mmol/g)
0	1	0.03	0.58
1	2	0.04	0.85
6	3	0.05	2.96
12	4	0.07	3.5
24	5 (SiO_2−Au)	0.09	4.77
24	6 (SiAu400)[a]	0.02	−
−	SiAuD1	0.091	−
−	SiAuD3	0.096	−
−	SiAuD6	0.081	−

[a] Refers to sample 5 heated at 400 °C.

The inset of Figure 1A shows pictures of (A) fumed silica sample 5 before immersion in $HAuCl_4$ solution, (B) sample 5 after immersion in $HAuCl_4$ solution for 40 h, (C) the fumed silica−gold nanocomposite sample in B after being heated at 400 °C for 1 h, and (D) the Au nanoparticle−fumed silica (sample 5) material grown in the presence of 10^{-3} M dodecylamine. It can clearly be seen that, whereas the fumed silica sample is colorless, the other samples are colored, with colors ranging from blue (B) to a very light pink (D). These colors are clearly due to the presence of gold nanoparticles on the fumed silica surface and occur as a result of the excitation of surface plasmon vibrations in the gold nanoparticles.[12] Thus, $AuCl_4^-$ ions are spontaneously reduced in the presence of fumed silica, resulting in the formation of surface-bound gold nanoparticles. Colloidal gold solutions are normally ruby red in color under conditions where the particles are in a dispersed state.[12a,b] When the particles are close enough that there is overlap of the surface plasmon vibrations between neighboring particles, the optical properties change, and the solution turns blue. Such changes in the optical properties of colloidal gold solutions have been used with success in monitoring the biotin−avidin interaction process,[12c] as well as the hybridization of DNA.[12d] Thus, the blue color in the sample 5−gold nanocomposite materials indicates fairly close packing of the gold particles on the silica surface. On heating, the composite turns to a light red color (inset of Figure 1A, picture C), which is indicative of reduced packing of the gold particles. This might occur by either aggregation of gold particles, leading to an effective increase in the average interparticle distance, or by desorption of weakly bound gold nanoparticles on the surface of the fumed silica. We strongly believe the latter mechanism is operative

(11) Fripiat, J. J.; Uytterhoeven, J. *J. Phys. Chem.* **1962**, *66*, 800.

(12) (a) Storhoff, J. J.; Lazarides, A. A.; Mucic, R. C.; Mirkin, C. A.; Letsinger, R. L.; Schatz, G. C. *J. Am. Chem. Soc.* **2000**, *122*, 4640. (b) Reynolds, R. R., III; Mirkin, C. A.; Letsinger, R. L. *J. Am. Chem. Soc.* **2000**, *122*, 3795. (c) Sastry, M.; Lala, N.; Patil, V.; Chavan, S. P.; Chittiboyina, A. G. *Langmuir* **1998**, *14*, 4138. (d) Elghanian, R.; Storhoff, J. J.; Mucic, R. C.; Letsinger, R. L.; Mirkin, C. A. *Science* **1997**, *277*, 1078.

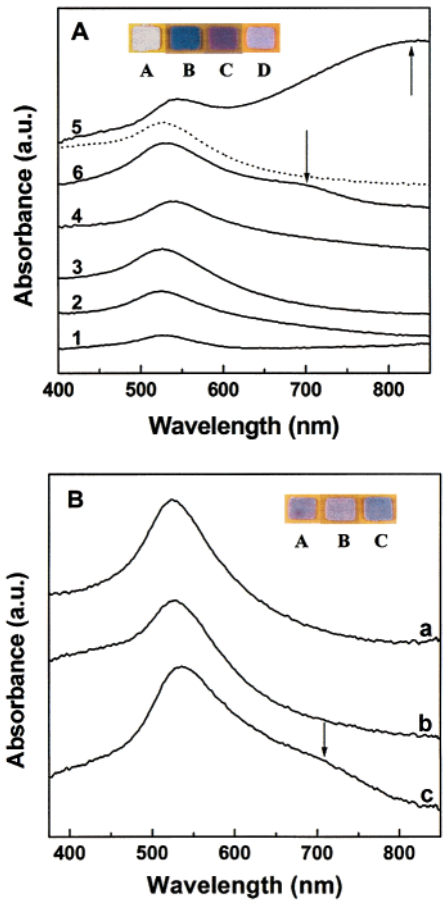

Figure 1. (A) UV−vis spectra recorded from fumed silica samples 1−5 after spontaneous reduction of $AuCl_4^-$ ions. The numbers of the samples are indicated next to the respective curves. The spectrum recorded from the sample 5−gold nanoparticle material after heat treatment (spectrum 6) is also shown. The dotted curve indicates the spectra of the sample 5−gold nanocomposite material grown in the presence of 10^{-3} M dodecylamine. The inset shows pictures of (A) fumed silica sample 5 before immersion in $HAuCl_4$ solution, (B) sample 5 after immersion in $HAuCl_4$ solution for 40 h, the fumed silica−gold nanocomposite sample in B after being heated at 400 °C for 1 h, and (D) the Au nanoparticle−fumed silica (sample 5) material grown in the presence of 10^{-3} M dodecylamine. (B) UV−vis spectra recorded from the Au nanoparticle−fumed silica (sample 5) materials grown in the presence of dodecylamine molecules of concentrations (a) 10^{-1}, (b) 10^{-3}, and (c) 10^{-6} M. The inset shows pictures of the Au nanoparticle−fumed silica sample 5 materials grown in the presence of dodecylamine molecules of concentrations (A) 10^{-1}, (B) 10^{-3}, and (C) 10^{-6} M.

as EDX measurements of the concentration of gold on silica after heat treatment yielded a decrease in the Au/Si weight ratio (Table 1, samples 5 and 6). The results of thermogravimetric analysis to be presented later support this contention. The light pink color of the Au nanoparticle−fumed silica sample 5 (inset of Figure 1A, picture D) grown in the presence of 10^{-3} M dodecylamine molecules also indicates much smaller, well-dispersed gold nanoparticles on the surface of fumed silica. The separation between the gold nanoparticles in this case is possibly stabilized by a monolayer of dodecylamine molecules bound to the surface of the gold nanoparticles.

More precise changes in the optical properties of the different fumed silica samples after formation of the gold nanoparticles by spontaneous reduction of $AuCl_4^-$ ions were monitored by UV−vis spectroscopy. Figure 1A shows the spectra recorded from samples 1−5 (curves 1−5, respectively) and the sample 5−gold nanocomposite material after heat treatment (curve 6), as well as the sample 5−gold nanocomposite material grown in the presence of 10^{-3} M dodecylamine (dotted curve). A strong absorbance in the visible region of the electromagnetic radiation (around 520−540 nm, due to the excitation of surface plasmon vibrations)[12] is observed for all the fumed silica samples and is responsible for the pink and blue coloration of the composite materials. Whereas the optical properties of the fumed silica−gold nanoparticle composite materials are essentially the same for samples 1−4 (curves 1−4), sample 5 shows the presence of an additional band at ca. 820 nm (curve 5). Furthermore, upon heating of the fumed silica−gold nanocomposite material, this band shifts to the blue to a value of ca. 725 nm (curve 6). The higher-wavelength features in spectra 5 and 6 are attributed to excitation of longitudinal surface plasmon vibrations and are a consequence of the close packing of the gold nanoparticles in the silicate matrix.[12] It is also well-known that a red shift in the longitudinal plasmon vibration is an indication of the extent of aggregation of the nanoparticles.[13] The above results can be interpreted as follows. Even though the surface concentration of free hydroxyl groups increases monotonically for fumed silica samples 1−5 (Table 1), close packing (in terms of overlap of plasmon vibrations in the gold particles) occurs only above a critical hydroxyl group concentration, which is reached in the case of sample 5. The shift in the longitudinal plasmon resonance from 820 nm for the fumed silica sample 5−gold nanocomposite material to 725 nm upon heating of the sample indicates disruption in the close packing of the gold nanoparticles on the fumed silica surface. This might arise as a result of the desorption of loosely bound gold nanoparticles, as briefly mentioned earlier. The fumed silica sample 5−gold nanomaterial grown in the presence of 10^{-3} M dodecylamine molecules shows only a single resonance centered at 520 nm (dotted curve, Figure 1). Although this indicates that the gold nanoparticles on the surface of the fumed silica are well separated, a firm statement on the size of the nanoparticles thus formed cannot be made on the basis of UV measurements alone.

The inset of Figure 1B shows pictures of Au nanoparticle−fumed silica sample 5 composites grown in the presence of dodecylamine molecules of concentrations (A) 10^{-1} M, (B) 10^{-3} M, and (C) 10^{-6} M. From the pictures, it can clearly be seen that the color gradually changes from purple to light pink as the concentration of dodecylamine is increased from 10^{-6} to 10^{-1} M. This variation in color certainly arises from the different sizes of the gold nanoparticles. That this is indeed true is borne out by the EDX measurements performed on the gold nanoparticles grown in the presence of dodecylamine (Table 1, samples SiAuD1−3), which show that the Au/Si weight ratio is essentially constant for the three concentrations of amine in solution. Therefore, the change in optical properties for these three materials

(13) (a) Blatchford, C. G.; Campbell, J. R.; Creighton, J. A. *Surf. Sci.* **1982**, *120*, 435. (b) Kreibig, U.; Genzel, L. *Surf. Sci.* **1985**, *156*, 678.

must be attributed to size-dependent variations in the electronic structure and not to nanoparticle packing considerations.

Figure 1B shows the UV−vis spectra recorded from the fumed silica sample 5−gold nanocomposite material grown in the presence of different concentrations of dodecylamine, viz., (a) 10^{-1}, (b) 10^{-3}, and (c) 10^{-6} M. A strong absorbance in the 520−540 nm region is observed for these samples also. Further, an additional band at ca. 710 nm is observed for sample SiAuD6, which again can be attributed to excitation of longitudinal surface plasmon vibrations resulting from the close packing of gold nanoparticles in the siliceous matrix. Previously, it was stated that close packing occurs only above a critical hydroxyl group concentration that was achieved in case of Au nanoparticle−fumed silica sample 5, for which, we recollect, an additional band at ca. 820 nm was observed. The shift in the longitudinal plasmon resonance from 820 to 710 nm for the SiAuD6 sample indicates a disruption of the close packing, which might be due to the formation of self-assembled monolayers of dodecylamine over the surface of the gold nanoparticles and the separation of the nanoparticles on the surface of the fumed silica.

The UV−vis results clearly point to the important role played by the hydroxyl groups on the surface of the fumed silica samples in the reduction of $AuCl_4^-$ ions. It is pertinent to mention here the work of Esumi et al.,[6a] who recently demonstrated the spontaneous reduction of $AuCl_4^-$ ions by "sugar balls" [sugar persubstituted poly(amidoamine) dendrimers]. They showed that the reduction of the metal ions is due to free hydroxyl groups on the sugar moieties in the dendrimer.[6a] We believe a similar mechanism is operative here, with the silanol groups on the silica surface participating in the reduction of the chloroaurate ions, followed by stabilization of the gold nanoparticles thus formed on the silica surface. Further details of the exact mechanism leading to the reduction of $AuCl_4^-$ ions are being worked out and will be addressed in future communications. Indeed, another important issue to be addressed is the nature of the interaction of the gold nanoparticles with the fumed silica surface, which is also currently being studied. In this regard, we mention that, when an oxide such as silica is desired as a support for some metal, the oxide should have a specific surface area ranging from 100 to 700 $m^2\ g^{-1}$.[14] The fumed silica material used here has a specific surface area of 384 $m^2\ g^{-1}$, which can serve the purpose of a good support for gold nanoparticles excellently. The higher concentration of hydroxyl groups in sample 5 leads to a higher density of gold particles on the fumed silica surface and to important changes in the optical properties of the nanocomposite (Figure 1A), thereby supporting the contention that the silanol groups are responsible for the reduction of $AuCl_4^-$ ions.

The sizes of the gold nanoparticles formed on the surface of fumed silica sample 5 before heating and of the Au nanoparticle−fumed silica samples grown in the presence of dodecylamine molecules were estimated by transmission electron microscopy measurements. Figure

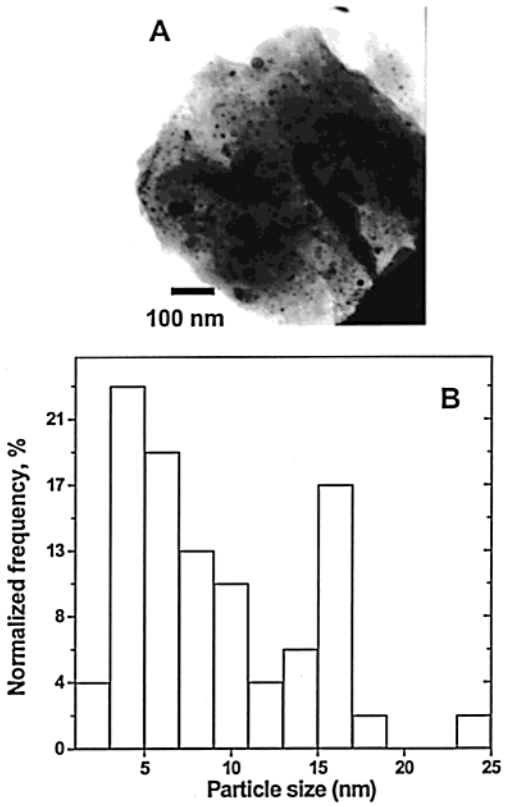

Figure 2. (A) TEM image of fumed silica sample 5 after spontaneous reduction of the $AuCl_4^-$ ions. (B) Particle size histogram from an analysis of the gold nanoparticles shown in Figure 2A.

2A shows the TEM image recorded from fumed silica sample 5 after spontaneous reduction of the $AuCl_4^-$ ions. One can clearly see a number of gold nanoparticles, which range in size from 2 to 30 nm. The sizes of the nanoparticles were analyzed from this image, and the particle size histogram is plotted in Figure 2B. It was observed that the particle size distribution was broad, with some indication of bimodality. The smaller-sized particles were found to have an average size of ca. 7 nm, while the larger particles were ca. 16 nm in dimension. Fairly dense packing of the gold nanoparticles can be seen, thus supporting the UV−vis results presented earlier (Figure 1A). Selected area diffraction measurements (data not shown) clearly indicated the formation of nanocrystalline gold particles on the surface of fumed silica.

Figure 3A shows a low-magnification TEM image recorded from the Au nanoparticle−fumed silica sample 5 material grown in the presence of 10^{-3} M dodecylamine. Figure 3B shows a series of four magnified TEM images recorded from the same sample. From a comparison with the TEM image recorded from the nanocomposite grown without dodecylamine molecules in solution (Figure 2A), it can be seen that the gold nanoparticles grown in the presence of amine molecules are smaller. A gold nanoparticle diameter of ca. 3.5 ± 0.5 nm was estimated from an analysis of the TEM images shown in Figure 3B. It is clear that the dodecylamine molecules present in solution during the reduction of the gold ions by fumed silica significantly reduce the size of the nanoparticles formed and lead to a more monodisperse particle size distribution. This presumably occurs through the formation of a self-

(14) Bond, G. C. *Handbook of Heterogeneous Catalysis*; Ertl, G., Knözinger, H., Weitkamp, J., Eds.; VCH: Weinheim, Germany, 1997; Vol. 2, Section 3, pp 752−770.

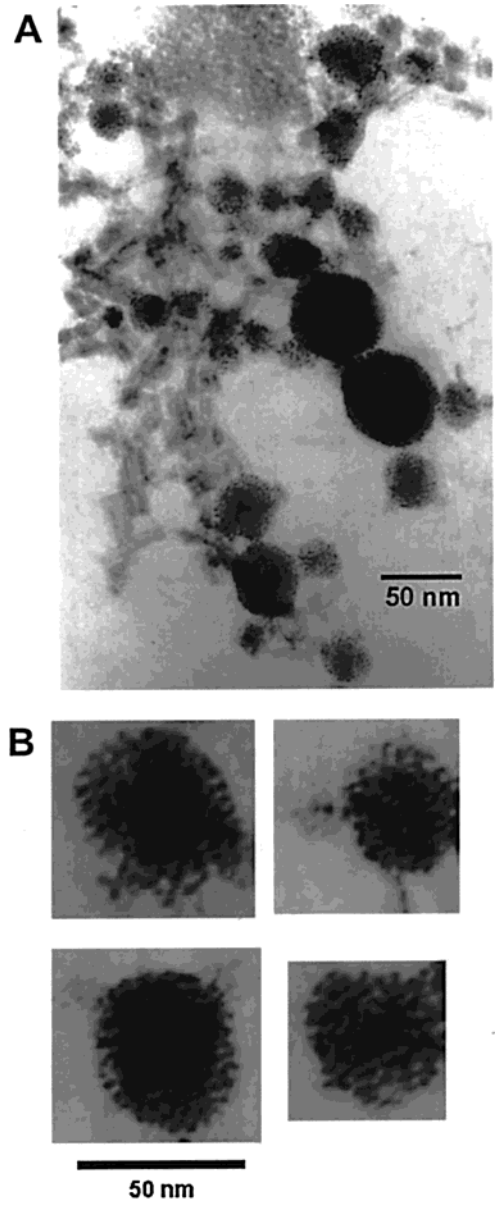

Figure 3. (A) TEM image recorded from fumed silica sample 5 after spontaneous reduction of the $AuCl_4^-$ ions in the presence of 10^{-3} M dodecylamine. (B) Series of four magnified TEM images recorded from the same sample.

assembled monolayer of amine molecules on the surface of the gold nanoparticles during the initial nucleation and growth of the nanoparticles. The dodecylamine monolayer thus limits the growth of the nanoparticles and stabilizes the particle size distribution, which is an important result of this investigation.

The sizes of the gold nanoparticles were also estimated from the X-ray diffraction line width broadening of the (111) Bragg reflection of gold by applying the Debye−Scherrer formula.[15] Figure 4A shows the XRD patterns in the 2θ range 36−40° recorded from Au nanoparticle−fumed silica sample 5 composites grown in the presence of dodecylamine molecules of concentrations (a) 10^{-1}, (b) 10^{-3}, and (c) 10^{-6} M. It also shows the XRD patterns for (d) composites grown in the absence of dodecylamine and (e) this sample after being heated at 400 °C for 1 h. The (111) Bragg reflection from the gold nanoparticles at $2\theta = 38.2°$ is clearly observed in the patterns for all of the samples. From the broadening of the (111) reflection in the XRD patterns, the sizes of the gold particles were estimated (listed in Table 2). It can be seen that the width of the Bragg reflection is considerably reduced after the heat treatment (compare curves d and e, Figure 4A). This indicates sintering of the gold nanoparticles upon heating at 400 °C and is a result that cannot be inferred from UV−vis spectroscopy measurements alone, which only indicated a reduction in the density of the gold nano-

(15) Jeffrey, J. W. *Methods in Crystallography*; Academic Press: New York, 1971.

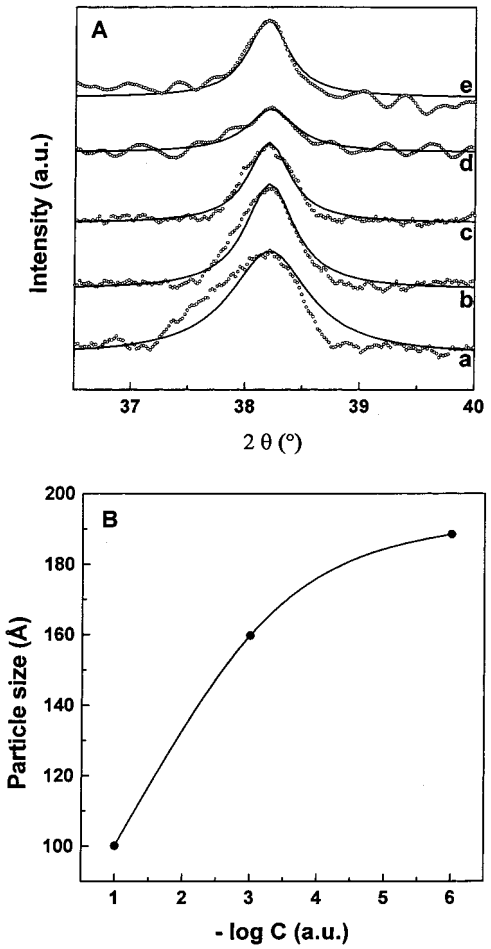

Figure 4. (A) XRD patterns recorded from the Au nanoparticle−fumed silica sample 5 materials grown in the presence of dodecylamine molecules of concentrations (a) 10^{-1}, (b) 10^{-3}, and (c) 10^{-6} M; (d) from the material grown in the absence of dodecylamine; and (e) from the sample in part d after being heated at 400 °C for 1 h. Solid lines indicate Lorentzian fits of the respective curves. (B) Dependence of Au nanoparticle size on concentration (C) of dodecylamine in solution (plot of particle size vs $-\log C$).

Table 2. Results of Cyclohexene Hydrogenation

conc of DDA solution (M)	catalyst	size of Au nanoparticles (nm)	conversion of cyclohexene (mol %)	selectivity of cyclohexane (%)
−	SiO_2−Au[a]	17	73	100
−	SiAu400[b]	21	>99	100
10^{-1}	SiAuD1	10	>99	100
10^{-3}	SiAuD3	16	86	100
10^{-6}	SiAuD6	19	82	100

[a] Refers to autoreduced gold sample 5 (24 h HCl treatment of fumed silica). [b] Refers to the sample heated at 400 °C (sample 6, Table 1).

Table 3. Comparison of Catalytic Activity of Au Nanoparticle−Fumed Silica Composites with Earlier Results

substrate	substrate pressure (psi)	H_2 pressure (psi)	reactor type	reaction temp (°C)	reaction time (min)	conversion (mol %)	ref
cyclohexene	−	200	pressure autoclave	80	90	>99	this work
1-pentene	0.023	14.6	fixed-bed down-flow reactor	100	90	10	16a
propane	0.38	5.8	U-shaped batch reactor	150	80	11	16b

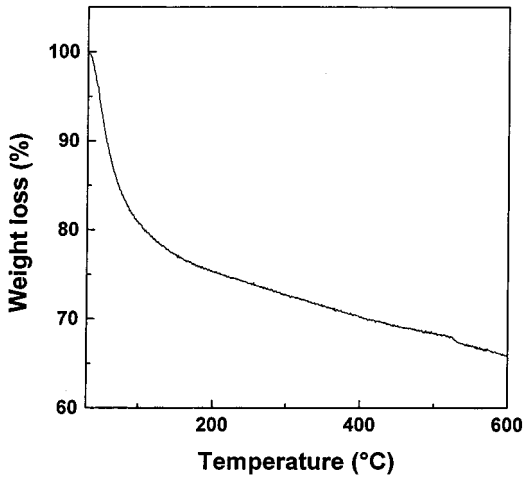

Figure 5. TGA data recorded from Au nanoparticle−fumed silica sample 5 after spontaneous reduction of the $AuCl_4^-$ ions.

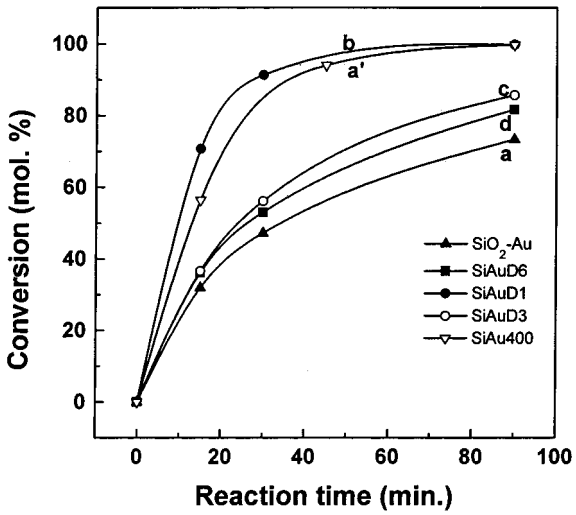

Figure 6. Conversion (in mole percent) vs reaction time (in minutes) plots for cyclohexene hydrogenation using the following catalysts: (a) SiO_2−Au, (a′) SiAu400, (b) SiAuD1, (c) SiAuD3, and (d) SiAuD6.

particles on the fumed silica surface after the annealing process.

Comparing the broadening of curves a−c in Figure 4A (Au nanoparticle−fumed silica sample 5 grown in the presence of dodecylamine of concentrations 10^{-1}, 10^{-3}, and 10^{-6} M, respectively) it can be inferred that the size of the gold particles is dependent on the concentration of dodecylamine molecules. The dependence of the Au nanoparticle size on the concentration (C) of dodecylamine is displayed in Figure 4B, where the particle size (in Å) is plotted against $-\log C$. From the curve, one can conclude that the particle size increases with increasing value of $-\log C$ (i.e., with decreasing concentration of dodecylamine) and eventually reaches a stable value.

Thermogravimetric (TGA) measurements were performed at a heating rate of 10 °C/min. The TGA data for the Au nanoparticle−fumed silica sample 5 material after spontaneous reduction of the chloroaurate ions are plotted in Figure 5. A large weight loss, corresponding to ca. 20% of the overall sample weight, is observed at ca. 100 °C and is attributed to the loss of adsorbed water in the sample. However, a fairly steady decrease in mass is observed up to 600 °C and amounts to a further 13% weight loss. This loss is attributed to desorption of weakly bound gold nanoparticles on the fumed silica surface and agrees with the EDX (Table 1, samples 5 and 6) and UV−vis results, which indicated a reduced packing density of the gold particles after heating (Figure 1A, compare curves 5 and 6).

The Au nanoparticle−fumed silica samples synthesized from sample 5 in the presence or absence of dodecylamine and after heat treatment were tested for catalytic activity in the hydrogenation of cyclohexene. The results of the hydrogenation reaction are summarized in Table 2, and the conversion of cyclohexene vs reaction time is plotted in Figure 6. It can be observed that the heated sample (cyclohexene conversion > 99%) shows better activity than the as-prepared sample 5−Au nanoparticle material (cyclohexene conversion = 73%). The better activity of the heated sample might be due to the reduction in density of the gold nanoparticles on the silica surface (as indicated by the UV−vis, EDX, and TGA results), thus leading to a more facile reaction of cyclohexene with H_2. Further, for the Au−SiO_2−DDA samples, the highest catalytic activity is observed in the case of sample SiAuD1 (cyclohexene conversion > 99%), and the activity increases in the order SiAuD6 < SiAuD3 < SiAuD1. This increase in catalytic activity can be correlated with the particle size of each sample (calculated from the XRD line width at $2\theta = 38.2°$) given in Table 2. It is evident that the activity increases with decreasing particle size, as smaller-sized particles have more surface area and allow more space for the reactant molecules to become adsorbed onto the surface. It is known from the literature that gold supported on silica is a good catalyst for the hydrogenation of unsaturated hydrocarbons at moderate temperatures and pressures,[16] the reaction rate being dependent on the particle size and gold concentration. The few results available in the literature are summarized in Table 3. From these results, it can be ascertained that the catalytic activity of our Au−SiO_2 composite catalyst system is comparable to the activities of the systems studied earlier.

(16) (a) Sermon, P. A.; Bond, G. C.; Wells, P. B. *J. Chem. Soc., Faraday Trans. 1* **1979**, *75*, 385. (b) Saito, S.; Tanimoto, M. *J. Chem. Soc., Chem. Commun.* **1988**, 832.

We also mention two studies on the hydrogenation of cyclohexene, one using gold powder[17] and another using gold films[18] at 196−342 °C. In both cases, the dehydrogenation product (benzene) and the hydrogenation product (cyclohexane) were formed. The selectivity of the former increased with increasing temperature and with decreasing hydrogen pressure. In our study, 100% selectivity for the hydrogenated product (cyclohexane) was observed for all of the reactions.

Conclusion

In conclusion, it has been shown that gold nanoparticles can be obtained by the spontaneous reduction of aqueous chloroaurate ions by silanol groups present in fumed silica, thus leading to the formation of an inorganic−inorganic nanocomposite material. The fumed silica subsequently acts as a support for the nanoparticles thus formed. The size of the gold nanoparticles formed by the reduction of chloroaurate ions by fumed silica can be controlled by the addition of alkylamine molecules to the gold ion solution. The particle size is dependent on the concentration of alkylamine molecules. The sizes of the nanoparticles thus formed are commensurate with the range of gold nanoparticle sizes for which they show fairly good catalytic activity. This catalytic activity of the fumed silica−gold nanocomposite material was tested in the hydrogenation reaction of cyclohexene, where it was observed that the catalytic activity depends on the size of the nanoparticles. This opens up a new area for the application of inorganic−inorganic nanocomposites in catalysis and other future applications.

Acknowledgment. Two of us, C.R.P. and A.G., thank the Council of Scientific and Industrial Research, India, for research fellowships. The authors thank Mr. Debdut Roy for necessary assistance in the hydrogenation experiments.

CM010372M

(17) Chambers, R. P.; Boudart, M. *J. Catal.* **1966**, *5*, 517.
(18) Erkelens, J.; Kemball, C.; Galwey, A. K. *Trans. Faraday Soc.* **1963**, *59*, 1181.